IEEE Access
Multidisciplinary | Rapid Review | Open Access Journal

Received January 10, 2020, accepted January 16, 2020, date of publication January 22, 2020, date of current version January 30, 2020.

Digital Object Identifier 10.1109/ACCESS.2020.2968601

A Method for Detecting Rainfall From X-Band Marine Radar Images

YAN ZHENG[1], ZHEN SHI[1], ZHIZHONG LU[1], AND WENFENG MA[2]
[1]College of Automation, Harbin Engineering University, Harbin 150001, China
[2]FAWCar Company, Ltd., Changchun 130000, China

Corresponding author: Zhizhong Lu (luzhizhong@hrbeu.edu.cn)

This work was supported in part by the National Natural Science Foundation of China under Grant 11405035 and the Special Funding Project of Marine Nonprofit Industry Research under Grant 201405022-1.

ABSTRACT Currently, X-band marine radar images are commonly utilized to retrieve sea wave parameters. However, the marine radar image usually contains rainfall interference noise, which has an effect on the inversion accuracy of the wave parameters. To control the quality of the radar image when retrieving sea wave parameters, research on rainfall detection is investigated in this paper. Based on the correlation characteristics of the sea clutter and the difference in the correlation coefficients between sea wave images with and without rain, a novel method of rainfall detection is proposed. By analyzing the spatial and temporal correlation characteristics of sea clutter, the detection threshold of the proposed method is determined. To verify the effectiveness of the proposed method, X-band marine radar data collected at Pingtan, which is located on the coast of the East China Sea, are utilized in this paper. The experimental results demonstrate that the proposed method can effectively detect rainfall from X-band marine radar images.

INDEX TERMS Marine radar images, rainfall detection, correlation coefficient.

I. INTRODUCTION

Since X-band marine radar has the characteristics of high resolution, convenience, and low cost, it is commonly utilized for ship navigation. Meanwhile, X-band marine radar images contain abundant sea clutter information. Thus, X-band marine radar has the ability to measure the sea wave parameters. The high spatial and temporal resolution of marine radar compensates for the shortcomings of synthetic aperture radar (SAR) and high frequency (HF) ground wave radar [1], [2]. Research on retrieving sea wave information, such as the water depth, the sea surface current and the significant wave height, has attracted increasing attention in recent years [3]–[5].

When marine radar is utilized to monitor the sea surface, it mainly analyzes the backscatter echo signal received by the radar antenna. In addition to the sea clutter signal, the marine radar images also include various noises, such as the background noise, co-channel interference and rainfall. Because the backscatter mechanism is complex in the presence of rain, it is difficult to eliminate the rainfall interference from radar images [6]. A raindrop with a relatively large volume has a strong backscatter echo. Therefore, the echo intensity of a rainfall image will be stronger than that of a nonrainfall image under the same sea conditions. Meanwhile, the raindrops change the roughness of the sea surface and affect the propagation of the electromagnetic waves, which may not be able to reach the sea surface under heavy rainfall, meaning the sea surface cannot be normally observed by the radar system. Thus, the collected marine radar images in the presence of rain will contain substantial rainfall information. The rain interference changes the texture of the radar image, and the radar echo intensity is not uniformly distributed. Large differences exist in the echo intensity of the radar image contaminated by rain at a close range and a far range from the antenna.

By investigating the influence of rainfall on the echo characteristics of the sea surface, it is determined that the echo intensity of the radar image is proportional to the rainfall intensity [7]. The effects of artificial rain and wave speed on the radar echo image are studied [8]. The experimental results confirmed that the rainfall has an important effect on the measurement of sea waves. Although rainfall is a common meteorological phenomenon, the existence of rainfall interference has an effect on the radar imaging and leads to a deterioration of the retrieval accuracy for the sea wave parameters. Therefore, it is vitally important to detect rainfall

The associate editor coordinating the review of this manuscript and approving it for publication was Huimin Lu.

from X-band marine images before measuring the sea wave parameters.

Currently, due to a lack of reliable and quantitative experimental result regarding the interaction of sea surface scattering caused by rain and wind, research on the backscatter model of raindrops and sea waves in X-band radar images is rare. The mean and standard deviation of the radar images are used as the discriminate criteria for rainfall detection from the acquired X-band marine radar images [9]. Because of the complex influence of rainfall on the echo intensity, the mean and standard deviation parameters are not suitable for rainfall detection. Thus, the mean and difference coefficient of the sea surface echo intensity are used to detect rainfall from radar images [10]. However, the radar image during rain cannot be completely analyzed by the mean and difference coefficient parameters. The success rate of rainfall detection is limited, since the mean, variance, and difference coefficient cannot reflect the change in the sea surface texture, and these two-dimensional parameters are the local characteristics of the sea surface.

Since the zero pixel percentage (ZPP) of a rainfall image is usually smaller than that of an image in the absence of rain, the ZPP method has been proposed to detect a rainfall image from a radar image [11]. A hard threshold value is adopted to determine whether the radar image is contaminated by rain. The hard threshold value is useful for a case which heavy rainfall is detected. However, the accuracy of the ZPP method is limited, since the threshold value varies with different radar systems and it is difficult to determine without a sufficient amount of data. In practice, the threshold should be selected based on the environmental conditions, such as the distance from the radar antenna to the selected analysis area, and the radar parameters. The determination of the threshold is a topic to be further studied in the future. The one-dimensional continuous wavelet transform is utilized to correct the influence of rain on the X-band marine radar image [12]. For improving the retrieving accuracy of the wind information, the spatial texture differences between a radar image contaminated by rain and an image in the absence of rain are analyzed [13]. The rainfall detection of a radar image is mainly based on the assumption that rainfall in space is evenly distributed. However, local rainfall commonly exists in practice. In [14], based on the support vector machine technology, a method of detecting rainfall is proposed. The experimental results show that the proposed method has better detection performance than that of the ZPP method and can be applied to different radar systems directly.

References [15] and [16] indicate that sea clutter is associated in time and space and has correlation characteristics. To date, large amounts of research results regarding the correlation characteristics of sea clutter in time and space have been achieved [17]–[20]. In [17], the correlation feature is utilized to detect the target embedded in nonstationary sea clutter. The experimental results show that the detection performance can be improved by using the correlation feature of sea clutter. In [18], in order to model the sea clutter, a novel generalized autoregressive conditional heteroscedastic (GARCH) model for sea clutter modeling is proposed. A new model for the spatial correlation of sea clutter is proposed [19]. The required radar data of the S-band and C-band are used to verify the effectiveness of the proposed model. In [20], the sea clutter observed from airborne radar is investigated. In our investigation, it is determined that the correlation of marine radar image contaminated by rain is obviously different from that of a radar image in the absence of rain. Therefore, it is possible to detect a rainfall image based on the differences in the correlation characteristics.

To control the radar image quality and improve the retrieving accuracy of the sea wave parameters, a method of rainfall detection by using the difference in the correlation characteristics between a radar image contaminated by rain and an image in the absence of rain is proposed in this paper. The detection threshold is determined by analyzing the spatial and temporal correlation characteristics of sea clutter. Our primary goal is to propose a rainfall detection method that can effectively detect the rainfall from an acquired X-band marine radar image. The structure of the paper is as follows: Section II presents the correlation characteristics of the sea wave based on the X-band marine radar images. By utilizing the difference in the correlation characteristics between a radar image contaminated by rain and an image in the absence of rain, the proposed method of rainfall detection is illuminated in Section III. In Section IV, the effectiveness of the proposed method is verified based on the collected marine radar data. Finally, the conclusions are summarized in Section V.

II. THE SPATIAL AND TEMPORAL CORRELATIONS OF THE X-BAND MARINE RADAR IMAGE

The remote measurement of sea waves by using marine radar is based on the light and dark stripes in the radar image. The stripes are called sea clutter, and is formed by the backscattering of radar electromagnetic waves from the sea surface. In this section, we briefly review the correlation characteristics of sea waves.

The correlation characteristics of sea clutter include temporal and spatial correlations, which are associated in time and space [15], [16]. The temporal correlation, which usually reflects the fluctuation of sea clutter with time on the same radar resolution unit, is a fast descent process followed by a long attenuation process. The temporal correlation is also known as the interpulse correlation. However, the spatial correlation of the sea clutter is the correlation of the clutter at different distance and azimuth units. Research on the correlation characteristics of sea clutter is beneficial for detecting rainfall from X-band marine radar images. The Ice Multiparameter Imaging X-Band Radar (IPIX) data have been used to demonstrate that sea clutter has a long-time correlation at the second level and a short time correlation at the millisecond level [16], [19].

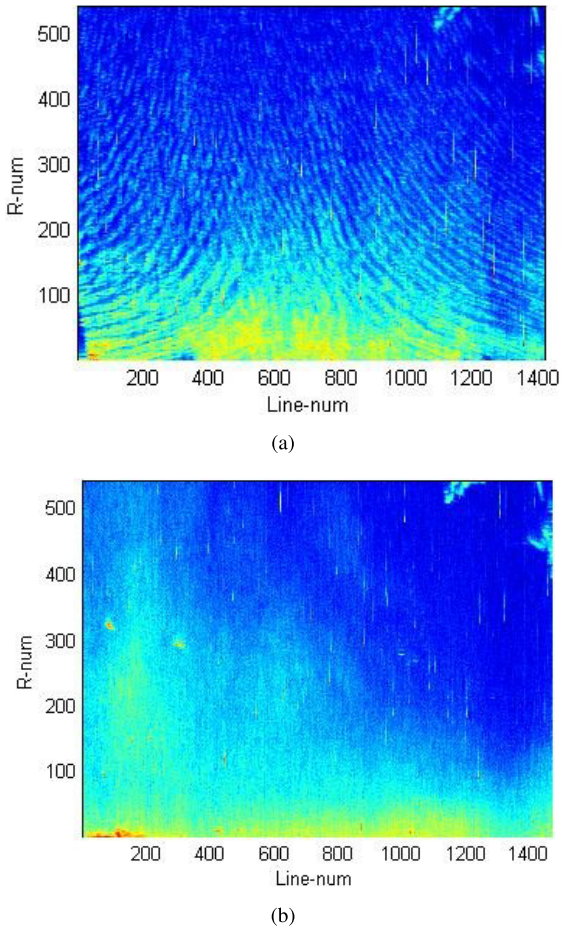

FIGURE 1. The marine radar images. (a) The radar image in the absence of rain; (b) The radar image contaminated by rain.

III. THE PROPOSED METHOD OF RAINFALL DETECTION BY UTILIZING THE DIFFERENCE IN THE CORRELATION CHARACTERISTICS

The selected marine radar images in the Cartesian coordinate system are shown in Fig. 1. From Fig. 1(a), we observed that the echo intensity of the radar image in the spatial domain is similar to the fluctuation of the sea level and shows a cyclical change in the radar image in the absence of rain. The horizontal coordinate denotes the number of sampling lines in the azimuth direction, and the vertical coordinate denotes the number of sampling points in the distance direction. Although the echo intensity of the sea clutter decays with distance, the variation of the echo intensity of the sea clutter in the azimuth direction is not distinct.

Because of the existence of rainfall noise, the scattering characteristics of sea clutter are changed. In the case of existing rainfall, rain appears in the radar image in the form of a speckle-like pattern, which is due to the uneven distribution of rainwater in a certain area under normal circumstances. As shown in Fig. 1(b), rainfall has the characteristics of high brightness and regional distribution in the original radar image, and the echo of the radar image obviously changes with the change of the rainfall intensity. In addition, we observed that the radar echo in the rainfall image is not uniformly distributed. The radar echo intensity also decays with the distance. The echo intensity is higher in the near range of radar image than that in the far range.

Compared to Fig. 1(a), a great difference also exists in the radar echo intensity in the azimuth direction. When a different analysis area is selected for the rainfall detection from the X-band marine radar image, the calculated ZPP will exhibit a substantial difference. Thus, the success rate of rainfall detection based on the ZPP method may depend on the analysis area selected.

The high-frequency components are introduced into the X-band marine radar images by the rainfall, resulting in changes in the correlation characteristics of the sea clutter. Rainfall and the raindrop size also have an effect on the horizontally polarized echoes produced by the raindrops splashing, which results in a texture change of the radar image.

Many mature research results related to the spatial and temporal correlations of sea wave have been obtained [18]–[20]. By utilizing the difference in the correlation characteristics between a radar image contaminated by rain and an image in the absence of rain, the research on rainfall detection is developed in this paper. By using the difference in the correlation characteristics, the flowchart for detecting rainfall from the X-band marine radar images is shown in Fig. 2. The detailed implementation process is as follows.

A. THE SELECTION OF THE ANALYSIS AREA

Due to the installation height restriction of the radar antenna, the main beam of the electromagnetic wave transmitted by the X-band marine radar is almost parallel to the sea surface when it grazes into the sea surface. The sea clutter intensity of the radar image decreases with an increase in the distance to the antenna. The actual radar image is generally distributed in the range of $1^\circ - 10^\circ$. In this paper, the sector image area $I_{sel}(r, \theta)$ is selected for a correlation coefficient analysis from the polar coordinate radar image, where r is the distance from the image pixel to the radar antenna and θ is the azimuth angle of the radar image. Meanwhile, in the near shore area, the radar image often contains ground clutter and the radar echo intensity can easily become saturated. When the selected analysis area is too far from the radar antenna, the radar receiver cannot receive the effective sea wave echo signal, since the echo signal is completely buried in the system noise. Based on the installation height h of the radar antenna, the texture characteristics of the sea clutter and the scope of the grazing incidence angle $\alpha \in (\alpha_d, \alpha_u)$, the boundary distance r_d and r_u can be achieved, where $r_d = \arctan(h/\tan\alpha_u)$ and $r_u = \arctan(h/\tan\alpha_d)$.

For shore-based radar, the echo area of the sea clutter can be observed from the collected radar image once the radar system is fixed. Thus, the boundaries θ_u and θ_d of the sea clutter in the azimuth direction can be determined.

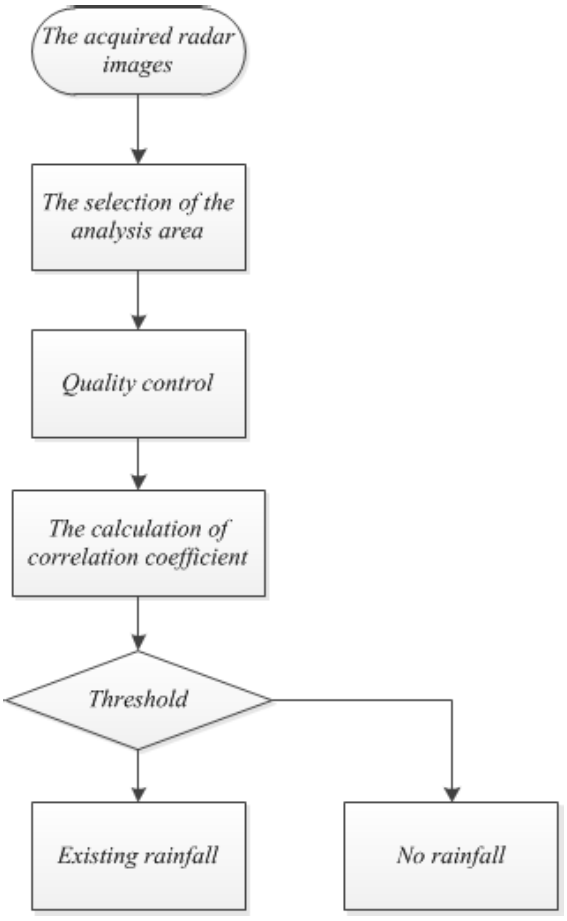

FIGURE 2. The flowchart of rainfall detection from X-band marine radar images.

B. QUALITY CONTROL

Under low sea conditions, the echo intensity of the radar image is mainly background noise. Thus, the strategy is used to control the quality of marine radar image and select the radar image with sea wave texture characteristics. In [21], the radar images that do not contain wave signatures and are contaminated by rain are discarded for retrieving wind information. Here, since the proposed method for rainfall detection is based on the sea clutter correlation characteristics, the radar images without a wave signature should be discarded.

In our experiment, a 14 bits digital acquisition card is used to collect the radar data. The gray value changes from 0 to 16383 and is mapped to an echo intensity from 0 to 2.5 V. Under low sea conditions, the system thermal noise is dominated in the acquired radar image. To control the image quality, a threshold of the thermal noise is adopted for rainfall detection. The threshold value is determined based on the thermal noise of the system. Based on the configuration parameters of the radar, thermal noise exists and is commonly less than 0.3 V. In our experiment, when the mean of the echo intensity of the selected analysis area is less than the threshold, the selected analysis area is not considered for calculating the correlation coefficient. The strategy of the quality control is given as

$$\begin{aligned} C_0 &: mean(I_{sel}(r,\theta)) > T_n \\ C_1 &: mean(I_{sel}(r,\theta)) \leq T_n \end{aligned} \tag{1}$$

where $mean(\cdot)$ denotes the mean value of the selected analysis area, T_n denotes the detection threshold for the thermal noise, C_0 denotes the case where the acquired radar image has a high echo intensity, and C_1 denotes the case where the selected radar image is acquired under low sea conditions and is considered as black without wave signature. In this paper, the radar image is discarded for rainfall detection, when the mean of the backscatter echo intensity of the analysis area is less than the threshold.

C. THE CALCULATION OF THE CORRELATION COEFFICIENT

When the radar image is contaminated by rain, the correlation characteristics of the radar echo can be described by the autocorrelation coefficient which is a mathematical quantity and measures the degree of correlation between two variables. The autocorrelation coefficient $\rho(\tau) \in [-1, 1]$ is given as

$$\rho(\tau) = \frac{E\{x(t+\tau)x(t)\}}{E\{|x(t)|^2\}} \tag{2}$$

where $E(\cdot)$ is the expectation of variable, $\tau > 0$ is the lagged number, and $x(t)$ is the echo intensity of the radar image. The correlation is greater when the autocorrelation coefficient $\rho(\tau)$ is closer to 1. Based on (2), the correlation coefficient of the radar image with respect to the distance and azimuth direction can be calculated.

D. THRESHOLD DESIGN

When taking the antenna rotation period of the X-band marine radar and the temporal correlation characteristics of the sea clutter into account, the radar data collected in our experiment cannot be used to analyze the temporal correlation of the sea clutter. Based on the pulse repetition rate of the X-band marine radar and the time interval in the azimuth direction, the analysis of the temporal correlation can be ignored. Here, the correlation of the sea clutter in the azimuth direction is characterized by the correlation coefficient. In addition, the radar data in the distance direction can be used to analyze the spatial correlation of the sea clutter, because the time interval in the distance direction is very short. Thus, the threshold could be determined based on the difference in the autocorrelation coefficient between the sea clutter with rainfall and the sea clutter without rainfall.

Fig. 3 is the autocorrelation coefficient of the radar images of Fig. 1. The blue solid line denotes the correlation coefficient of a radar image in the absence of rain, and the red dashed line denotes the correlation coefficient of a radar image that is contaminated by rain. From Fig. 3, we can observe that the autocorrelation coefficient in the azimuth direction of the radar image in the absence of rain is different from that of the radar image contaminated by rain. In addition, a radar image in the absence of rain has a stronger

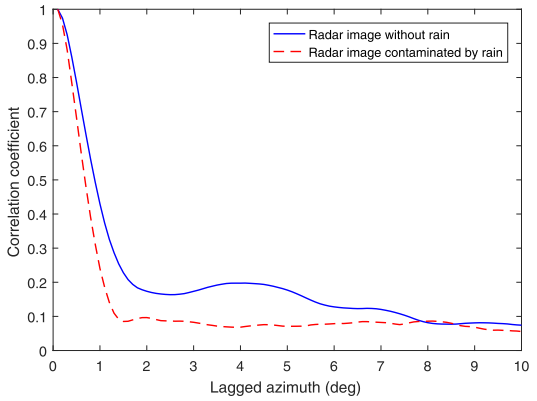

FIGURE 3. The autocorrelation coefficient of the radar image in the azimuth direction.

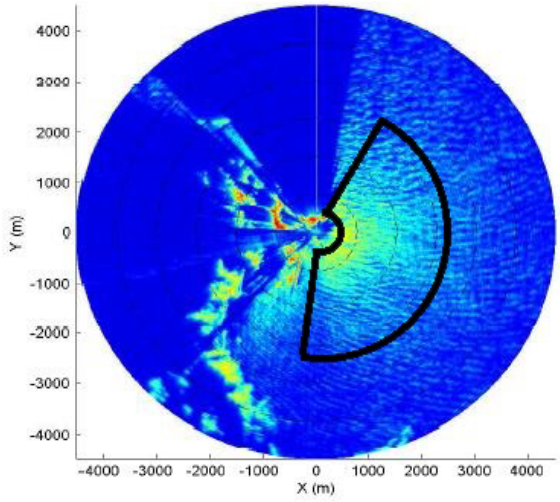

FIGURE 4. The collected marine radar image.

TABLE 1. The configuration of the X-band Marine radar.

Radar Parameters	The performance
Electromagnetic Wave Frequency	9.3 GHz
Antenna Angular Speed	22 r.p.m.
Antenna Height	45 m
Polarization	HH
Range Resolution	7.5 m
Horizontal Beam Width	0.9°
Vertical Beam Width	21°
Pulse Repetition Frequency	1300 Hz
Antenna Length	1.8 m
Pulse Width	50 ns

correlation than that of a radar image contaminated by rain. Hence, the threshold value could be determined based on the difference in the autocorrelation coefficient between the sea clutter with rainfall and the sea clutter without rainfall.

Based on the statistical analysis of the L-band radar data, it is shown that the correlation coefficient in the azimuth direction is not greater than the value 1/e when the separation in the azimuth direction is larger than the beam width [22]. The sea clutter can be considered to be uncorrelated, since its correlation coefficient is below 1/e, meaning the correlation of sea clutter is weak. By deeply investigating the correlation coefficient of the X-band radar image, we found that the correlation coefficient of sea clutter is greater than 1/e when the separation in the azimuth direction is less than the horizontal beam width. However, the correlation coefficient of the rain-contaminated radar image is less than 1/e. Thus, the task of rainfall detection from the X-band marine radar images can be completed by comparing the achieved correlation coefficient with the threshold value 1/e at the position of the horizontal beam width. When the autocorrelation coefficient of the radar image is lower than the threshold, the radar image is considered to be contaminated by rain; otherwise, it is considered to be without rain. The detection task can be shown as

$$H_0 : \rho \leq \gamma \quad v.s. \quad H_1 : \rho > \gamma \tag{3}$$

where γ is the threshold, H_0 denotes the case where the radar image is contaminated by rain, and H_1 denotes the case where the radar image is in the absence of rainfall. The lagged azimuth is different for different radar systems. The lagged azimuth of the sea clutter is related to the azimuth resolution of the radar antenna. In our radar system, the azimuth resolution is 0.9°. Based on the analysis of the acquired X-band marine radar images and the statistical analysis, we found that the correlation of sea clutter is larger than 1/e when the lagged azimuth is within the azimuth resolution. However, the correlation of a radar image contaminated by rain is less than 1/e. Since the rainfall echo of a radar image changes the correlation of the sea clutter, the correlation of a radar image contaminated by rain is different from that of a radar image in the absence of rain.

IV. EXPERIMENTAL RESULTS AND ANALYSIS

To verify the effectiveness of the proposed rainfall detection method, the spatial correlation characteristics of the sea clutter and the radar image contaminated by rain are investigated based on the acquired radar data.

A. THE EXPERIMENTAL DATA

Accumulated radar data from August 2013 at Pingtan, which is located on the coast of the East China Sea, were utilized to analyze and evaluate the validity of the proposed method. During the experiment, part of the acquired radar data are contaminated by rain.

In our experiment, the configuration of the X-band marine radar is given in Table 1. The original collected radar image is shown in Fig. 4. The echo intensity in the left part of the image is the ground clutter, which is not related to our research in this paper. The echo intensity in the right part is the sea clutter signal. The radar echo in the sector area selected by the black thick line is utilized for the correlation analysis.

The selected radar data contaminated by rain and the data in the absence of rain are shown in Fig. 5. The red dotted line denotes the radar data in the absence of rain and acquired

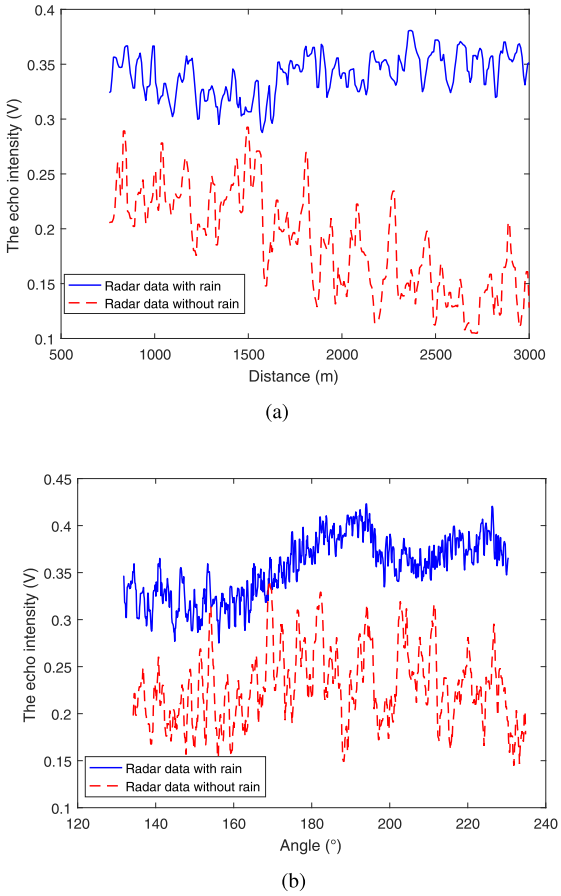

FIGURE 5. The X-band marine radar data in the respective distant and angular directions. (a) The selected data in the distance direction; (b) The selected data in the azimuth direction.

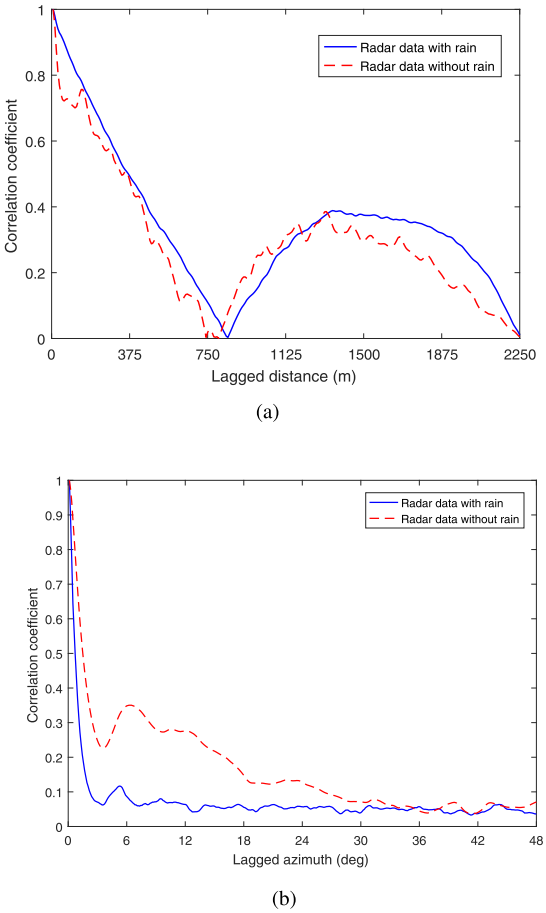

FIGURE 6. The correlation coefficient of the X-band marine radar images. (a) The correlation coefficient of the sampling points in the distance direction; (b) The average correlation coefficient of the sampling points in the azimuth direction.

before rainfall, while the blue solid line denotes radar data contaminated by rain and collected after rainfall. According to the on-site records, the heavy rain occurred. The mean of the radar echo contaminated by rain is relatively higher than that in the absence of rain. Fig. 5(a) shows the selected data in the distance direction at 160°. The horizontal coordinate denotes the distance and the vertical coordinate denotes the echo intensity. The distance from the radar antenna to the selected data is approximately 700 m. The selected data in the azimuth direction at a range of 1500 m are given in Fig. 5(b). The horizontal coordinate denotes the angle in the azimuth direction. The radar images acquired before and after rainfall are used to demonstrate the differences in the echo intensity.

B. EXPERIMENTAL RESULTS

The calculated correlation coefficients of the X-band marine radar image based on the proposed method are shown in Fig. 6. From Fig. 6(a), we observed that the difference in the correlation coefficient between the radar image contaminated by rain and the radar image in the absence of rain in the distance direction is slight. However, the correlation coefficient of the radar data in the absence of rain declines faster compared to that of the radar data contaminated by rain when the lagged distance is less than 75 m. The horizontal coordinate denotes the lagged distance in direction, and the vertical coordinate denotes the correlation coefficient. It is difficult to distinguish whether the radar images are contaminated by rain based on the correlation coefficient difference in the distance direction.

The differences in the correlation coefficients of the radar images in the azimuth direction are presented in Fig. 6(b). The horizontal coordinate denotes the lagged angle in the azimuth direction. We clearly observed that a large difference in the calculated correlation coefficient exists between the radar data contaminated by rain and the radar data in the absence of rain. The correlation coefficient of the radar data in the absence of rain is a fast descent process followed by a long attenuation process with fluctuation. The correlation coefficient of the radar data contaminated by rain is also a fast descent process when the lagged angle in the azimuth direction is less than 3°. Thus, a strong correlation of the sea clutter can be observed. When the lagged azimuth is greater than 3°, the correlation fluctuates and declines, which corresponds to a long-time weak correlation of the

sea clutter. Meanwhile, we observed that the correlation of the radar image contaminated by rain decreases faster than that of sea clutter at the lagged azimuth of approximately $0° - 3°$. Compared to the radar image in the absence of rain, the autocorrelation of the radar data contaminated by rain is weaker. From Fig. 6, we observed that the difference in the correlation coefficient in the distance direction is not obvious. However, a large difference exists for the correlation coefficients in the azimuth direction between the radar image in the absence of rain and the radar image contaminated by rain. Therefore, the correlation coefficient in the azimuth direction is calculated for rainfall detection in our experiment. Meanwhile, the threshold of the proposed rainfall detection method can be determined based on the difference in the correlation coefficient in the azimuth direction.

Based on the configuration of the X-band marine radar and the spatial characteristics of the sea clutter in the azimuth direction, we observed that the sea clutter has a long-time correlation at the second level and has a short-time correlation at the millisecond level. By comparison, we found that the radar image in the absence of rain has stronger short-time characteristics than that of the radar data contaminated by rain. In addition, a correlation difference fluctuation exists in our experiment. Thus, the detection threshold can be determined, and the rainfall detection can be completed based on the difference in the autocorrelation coefficient between a radar image contaminated by rain and an image in the absence of rain. Based on the experimental statistics, the correlation coefficient 1/e of the radar image at a lagged azimuth 0.9° (approximately 6 ms) is utilized as the detection threshold of the proposed method.

Reference [11] shows that radar images with the ZPP less than 50% are considered to be contaminated by rain. In our experiment, a correlation coefficient of the radar images less than 1/e at the lagged azimuth of 0.9° is considered to be contaminated by rain. Radar data acquired continuously on August 21, 2013 were utilized for the following analysis. During this period, the recorded radar data contain the rainfall intensity change process from sprinkling to heavy rain. The average wind direction and wind speed are 26° and 11 m/s, respectively. Moreover, the sector region of the radar image from 30° to 180° in the azimuth direction and from 400 m to 2500 m in the distance direction away from the radar antenna is utilized to obtain the correlation coefficient. We calculate the correlation coefficient based on the radar data from 30° to 180° at each fixed radial distance. Then, the averaged correlation coefficient is determined by averaging the achieved correlation coefficient at each range. In this paper, the averaged correlation coefficient is used for rainfall detection. The detailed performance based on the ZPP method and the proposed method is investigated below.

The selected analysis area and the calculated results of the X-band marine radar image in the absence of rain are presented in Fig. 7. Fig. 7(a) shows the selected analysis area from the radar image. A sea wave appears as stripes between light and dark in the marine radar image. After several seconds, it begins to rain. Fig. 7(b) is the calculated statistical histogram of the radar echo intensity based on the data in Fig. 7(a). The average correlation coefficient calculated by the radar image in the azimuth direction is shown in Fig. 7(c). Commonly, the co-channel interference of the

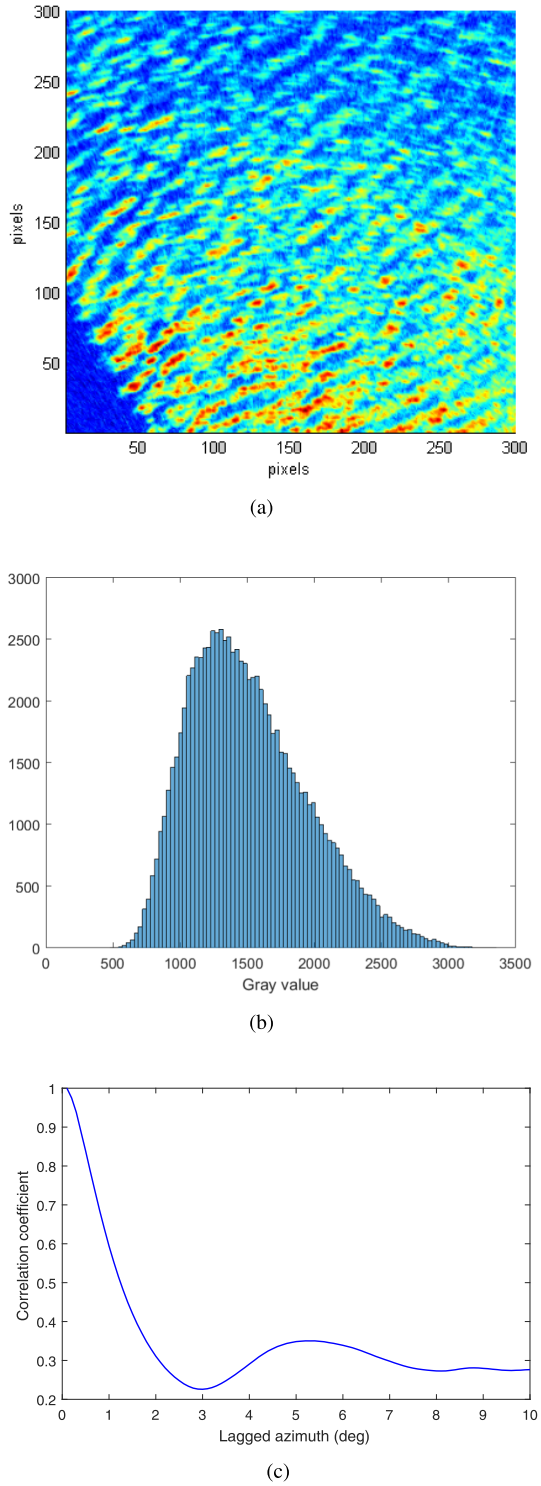

FIGURE 7. The selected analysis area and the calculated results of the X-band marine radar image in the absence of rain.

radar image has a liner distribution along the range direction. In this paper, the correlation characteristics of sea clutter in the azimuth direction are utilized for rainfall detection. Therefore, the co-channel interference has little effect on the correlation coefficient for rainy days. According to Fig. 7(c), the correlation coefficient decreases to 0.6 at a lagged 1°. Since the resolution of the antenna is approximately 0.9° in the azimuth direction, the correlation coefficient between pulses is strong. The correlation coefficient then decreases to 0.24 at a lagged 3°. From a lagged 0° to 3°, the short time correlation of the sea clutter is also observed. We observed that the calculated correlation coefficient is greater than the detection threshold at the lagged azimuth. Thus, the radar image does not contain rainfall information based on the proposed detection method. For this radar image, the whole area of the right part is utilized to calculate the ZPP based on the ZPP method. The obtained ZPP is 38.7% and is less than the detection threshold value. In this case, the radar image is considered to be contaminated by rain based on the ZPP method. However, this finding is inconsistent with the actual rainfall situation. Therefore, the proposed correlation coefficient method for rainfall detection presents a significantly better performance than the ZPP method.

The calculated results of the X-band marine radar image contaminated by light rain are presented in Fig. 8. Fig. 8(a) shows the selected analysis area from the radar image, and Fig. 8(b) is the statistical histogram of the radar echo intensity of Fig. 8(a). In addition, the calculated average correlation coefficient of the radar image in the azimuth direction is given in Fig. 8(c). We clearly observe that the obtained correlation coefficient of 0.27 is lower than the threshold value. Based on the whole area of the right part of the image, the achieved ZPP 25.3% is also less than the detection threshold value. The ZPP method can thus accurately distinguish the rainfall image. In this case, the radar image is considered to be contaminated by rain, and both the ZPP method and the proposed method have the ability to detect the rainfall image when it is sprinkling.

The calculated results of the X-band marine radar image contaminated by heavy rain are presented in Fig. 9. Fig. 9(a) shows the selected analysis area from the radar image, and Fig. 9(b) shows the statistical histogram of radar echo intensity of Fig. 9(a). The calculated correlation coefficient of the radar image in the azimuth direction is given in Fig. 9(c). The obtained average correlation coefficient 0.21 at the lagged azimuth is also lower than the threshold value. For the corresponding radar image, the calculated ZPP is 0.42%. Both the ZPP method and the proposed method could accurately distinguish the rainfall image from the acquired X-band marine radar image which is contaminated by heavy rain.

The rainfall intensity gradually increases from Fig. 7 to Fig. 9. We observed that the mean of the statistical histogram of the radar echo intensity and the autocorrelation coefficient decrease with an increase of the rainfall intensity. In addition, we observed that the task of rainfall detection can be completed based on the difference in the correlation coefficients of the radar images. From Fig. 10, we observed that the change in the autocorrelation coefficient reflects the change of the rainfall intensity.

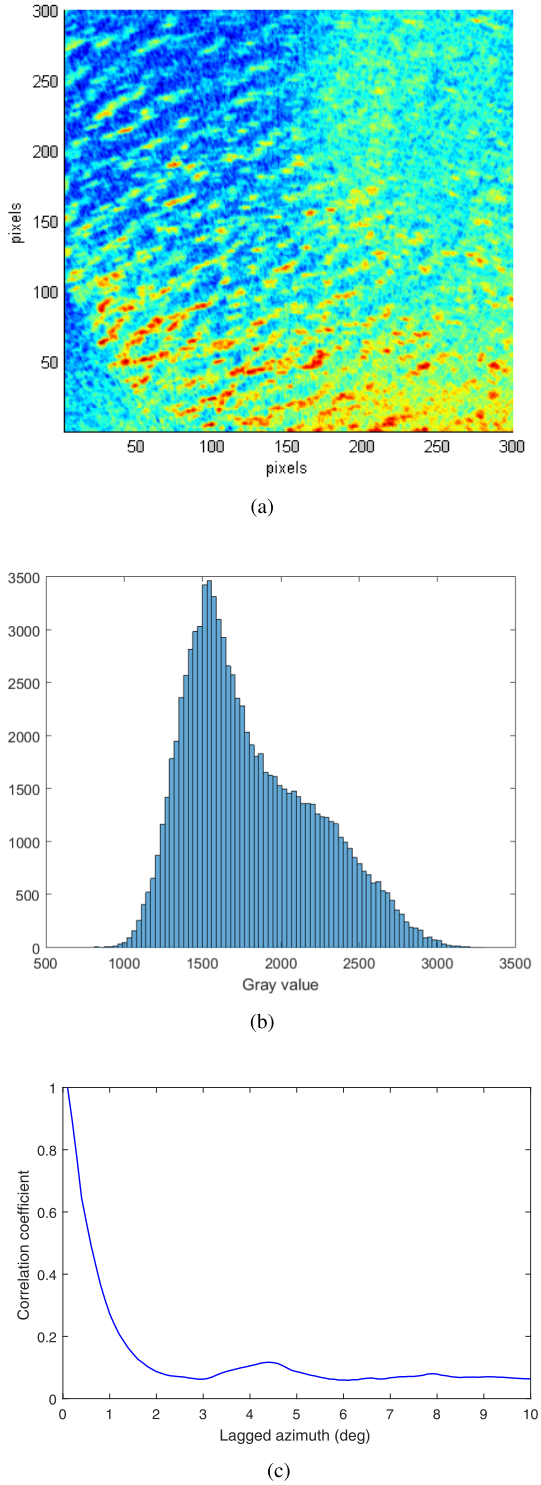

FIGURE 8. The selected analysis area and the calculated results of the X-band marine radar image contaminated by light rain. (a) The selected analysis area of the radar image; (b) The statistical histogram of the radar echo intensity; (c) The average correlation coefficient of the radar image in the azimuth direction.

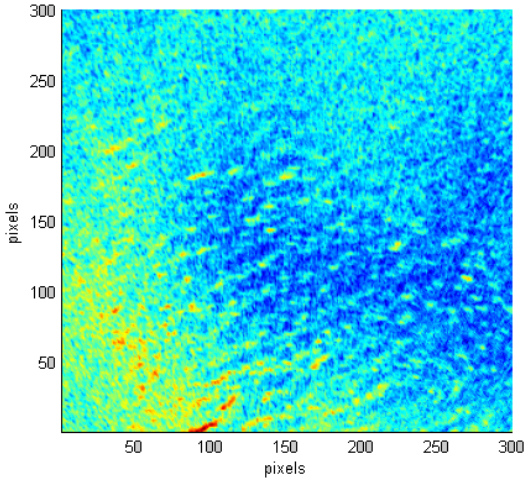

(a)

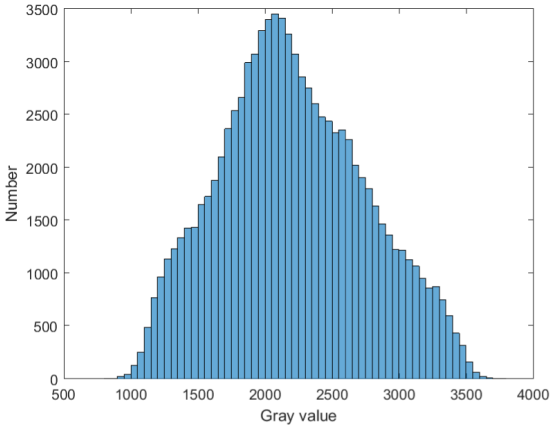

(b)

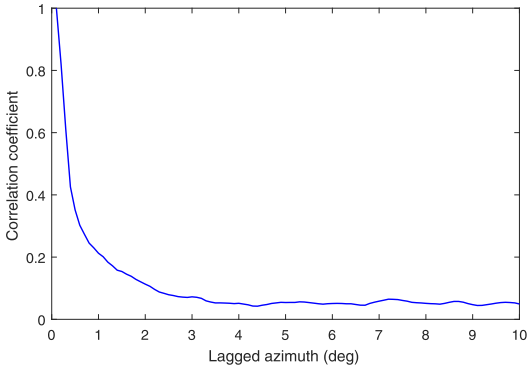

(c)

FIGURE 9. The selected analysis area and the calculated results of the X-band marine radar image contaminated by heavy rain. (a) The selected analysis area of the radar image; (b) The statistical histogram of the radar echo intensity; (c) The average correlation coefficient of the radar image in the azimuth direction.

Based on the above analysis, we found that the ZPP of the radar image decreases with an increase of the rainfall intensity. The results show that there is a significant difference

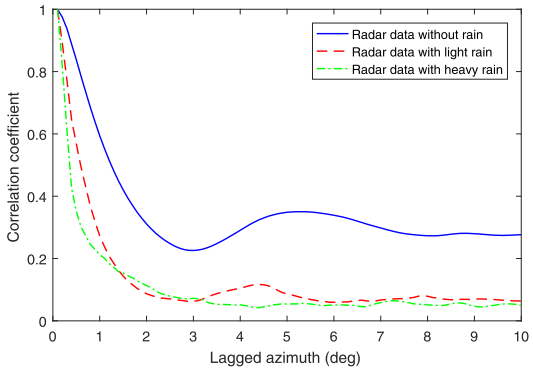

FIGURE 10. The correlation coefficient in the azimuth direction under different rainfall conditions.

between the radar image collected with rain contamination and the radar image in the absence of rain based on the ZPP method. The radar image before rainfall is determined to be a rainfall image based on the ZPP method. In addition, the correlation coefficient of the radar image also exhibits a significant difference between the image with rain contamination and the image without rain. The radar image can be accurately detected based on the proposed method of the correlation coefficient. Therefore, the correlation coefficient of the radar image can be used as a detection parameter to determine whether the radar image is contaminated by rain.

In addition, the success rate of rainfall detection of the proposed method compared to that of the ZPP method is also investigated. The X-band marine radar image system collects one image sequence every four minutes, and each image sequence contains 32 radar images. During the experiment, we selected the first image from the image sequence for rainfall detection. However, the partial radar data and the reference value were missed because of system failure. Here, we selected approximately 180 radar images on August 21 from 00:00 to 23:30 for rainfall detection. The simultaneous rain rate is recorded in the experiment and is adopted as the reference value. The rainfall gauge is installed in the observation area of the radar. The rain rate of the record is shown in Fig. 11. The blue solid line with stars denotes the rain rate. The unit of the rain rate data is mm/10 mins. However, the time interval of the selected radar image is four minutes. To minimize the error, the rainfall data are interpolated, where the interval after interpolation is also four minutes.

The rainfall detection performance of both the ZPP method and the proposed method is shown in Fig. 12. Fig. 12(a) shows the rainfall detection performance of the ZPP method. The blue solid line denotes the achieved ZPP, and the red solid line denotes the detection threshold of the ZPP method. The selected area with a green solid line denotes the radar image in the absence of rain. The time sequence denotes the acquired radar images during the process of rainfall. The rainfall detection performance of the proposed method is described in Fig. 12(b). The blue solid line denotes the achieved

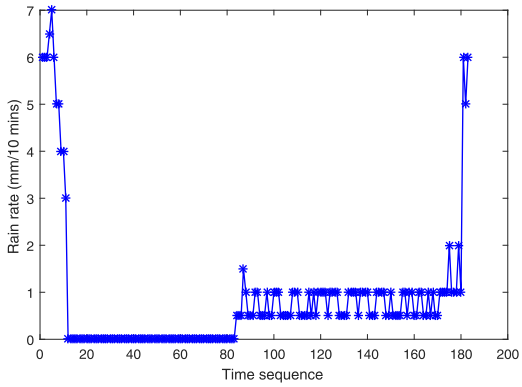

FIGURE 11. The rain rate recorded during the experiment.

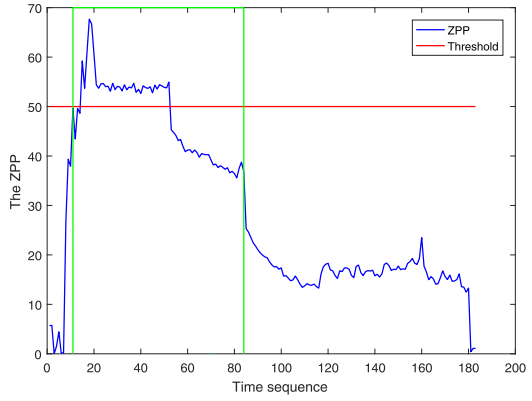

(a)

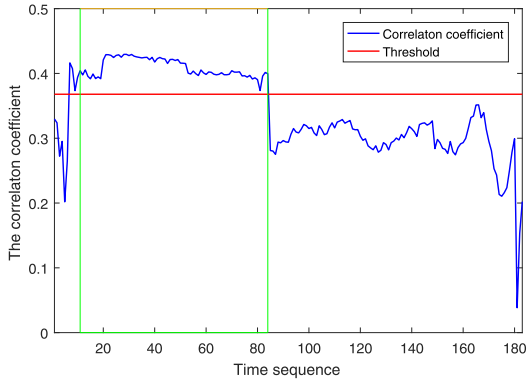

(b)

FIGURE 12. The rainfall detection of the X-band marine radar images. (a)The calculated ZPP of the radar images; (b) The calculated correlation coefficient of the radar images.

correlation coefficient with the proposed method, and the red solid line denotes the detection threshold. The green box denotes the radar image in the absence of rain. From Fig. 12, we observed that both the proposed method and the ZPP method present excellent detection performances for rainfall detection. Additionally, the success rate of rainfall detection is described based on the experimental results in Fig. 12, in order to demonstrate the effectiveness of the proposed method. Approximately 180 radar images are used for rainfall detection, of which 100 images contain rainfall information. The manual observation record of the ocean station is adopted as the true value. In this paper, the detection success rate refers to when the rain contaminated radar image is successfully detected as a rainfall image. Meanwhile, the false alarm is defined as when the radar image in the absence of rain is detected as a rainfall image.

The detection success rate of the proposed method is 96.4%. By investigating the experimental results, we found that the detection success rate of the ZPP method is close to 100% for the threshold value of 50%. Both the ZPP method and the proposed method can complete the task of rainfall detection. The detection success rate of the ZPP method is slightly higher than that of the proposed method. In Fig. 12(a), the green box denotes the radar image in the absence of rain. We observed that part of the ZPP of the radar image in the absence of rain is less than the detection threshold. However, from Fig. 12(b), we observed that almost all of the correlation coefficient in the green box is greater than the detection threshold. The false alarm rate of the ZPP method is approximately 40%. However, the false alarm rate of the proposed method is close to 0. Thus, the false alarm rate of the ZPP method is higher than that of the proposed method.

Since the threshold value of the ZPP method varies with different radar systems and is difficult to determine without sufficient data, the performance of the ZPP method is also discussed in this paper when the ZPP threshold value is set to 30%. In this case, the detection success rate of the ZPP method is 97.3%. Based on the determined detection threshold and the lagged azimuth, the detection success rate of the proposed method is 96.4%, and the false alarm rate of both methods is close to 0. Both the ZPP method and the proposed method can complete the task of rainfall detection and exhibit high detection performance. However, the proposed method has the advantage of determining the detection threshold without a sufficient amount of data compared to the ZPP method.

To better demonstrate the rain detection performance of the proposed method, a time sequence comparison between the detection performance of the ZPP and proposed methods as well as the rain rate data measured by the rain gauge is presented in Fig. 13. The x-axis denotes the time sequence, the left y-axis denotes the rain rate per 10 minutes, and the right y-axis denotes the achieved rainfall detection results from the acquired X-band marine radar images. A value of 1 represents a radar image that is contaminated by rainfall, and a value of 0 represents a radar image in the absence of rainfall. The blue solid line with stars denotes the rain rate, the green dotted line with crosses denotes the rainfall detection performance of the ZPP method, and the red solid line with circles denotes the detection performance of the proposed method. From Fig. 13, we observed that the proposed method can effectively detect rainfall from X-band marine radar images and has better detection performance than that of the ZPP method.

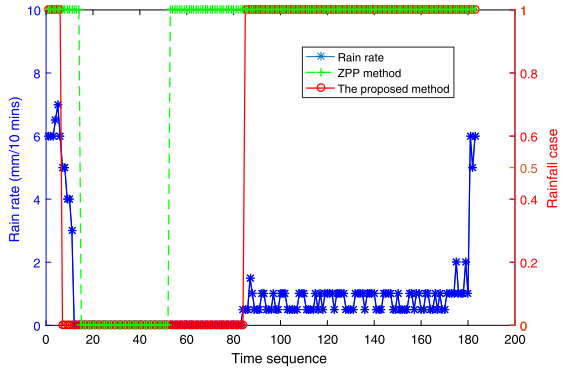

FIGURE 13. The time sequence comparison among the ZPP method, the proposed method and the rain rate.

In this paper, the detection threshold of the proposed method is obtained based on the spatial correlation characteristics of sea clutter in the azimuth direction and is independent of the environmental platforms. By using the measured radar data, the experiments describe that the proposed method has an approximately consistent detection performance compared to the ZPP method. Based on the above experiment and analysis, we determined that the proposed method is effective for detecting rainfall from X-band radar images.

Because of the installation height restriction of the X-band marine radar, the echo signal of the radar image from 400 m to 2500 m in the distance direction is selected for calculating the correlation coefficient, since the texture characteristics of the sea clutter are prominent. Commonly, the sea clutter can be considered to have a weak correlation when the correlation coefficient is less than 1/e. Under a low sea condition, the echo intensity of the sea wave will be misidentified as contaminated by rain, since the correlation of the sea clutter is very weak. In addition, in the case of a rainstorm, the coefficient correlation of a rainfall image may be higher than the detection threshold. In these cases, the performance of the proposed method will be seriously deteriorated. In our experiment, we found that the proposed method has a better detection performance than the ZPP method when the characteristics of sea wave are prominent when simultaneously accompanied by light rainfall. In this case, the rainfall has a strong effect on the correlation characteristics of the sea clutter. Therefore, in the future, the detection threshold of this method should be continually investigated under different sea conditions based on the difference in the correlation coefficients.

V. CONCLUSION

Currently, the required X-band marine images are typically utilized to retrieve the sea wave parameters. However, the reliability of the inversion results is low when radar images are contaminated by rain. Therefore, detecting rainfall from the collected X-band marine images is investigated in this paper. Although the ZPP method has the ability to detect rainfall from X-band marine radar images, it assumes that the rainfall is evenly distributed in the radar image. However, in practice, rainfall is unevenly distributed. The radar image before rainfall is easily determined to be contaminated by rain, due to the high detection threshold.

By analyzing the correlation characteristics of the radar image, the difference in the correlation coefficients between a radar image contaminated by rain and an image in the absence of rain is described in this paper. Then, a novel rainfall detection method based on the difference in the correlation characteristics is proposed. The effectiveness of the proposed rainfall detection method is verified based on the acquired marine radar data. The experimental results show that the proposed algorithm can not only accomplish the task of rainfall detection but also present a good performance compared to the ZPP method. Since the threshold value of the ZPP method is difficult to determine, the performance of the ZPP method is not optimal for a threshold value of 50%. The experimental results show that the proposed method also has a high detection rate by comparing the experimental results with the recorded rain rate data. Furthermore, the detection threshold and the lagged azimuth are determined in this paper, and a more accurate method for choosing the threshold and the lagged azimuth can be further investigated in the future. More experiments are needed to further verify and improve the effectiveness of the proposed rainfall detection method under different rainfall conditions.

REFERENCES

[1] I. R. Young, W. Rosenthal, and F. Ziemer, "A three-dimensional analysis of marine radar images for the determination of ocean wave directionality and surface currents," *J. Geophys. Res.*, vol. 90, no. C1, p. 1049, Feb. 2008.
[2] Y. Wei, Z. Lu, G. Pian, and H. Liu, "Wave height estimation from shadowing based on the acquired X-band marine radar images in coastal area," *Remote Sens.*, vol. 9, no. 8, p. 859, Aug. 2017.
[3] A. Wijaya, P. Naaijen, Andonowati, and E. V. Groesen, "Reconstruction and future prediction of the sea surface from radar observations," *Ocean Eng.*, vol. 106, pp. 261–270, Sep. 2015.
[4] W. Huang, X. Liu, and E. Gill, "Ocean wind and wave measurements using X-band marine radar: A comprehensive review," *Remote Sens.*, vol. 9, no. 12, p. 1261, Dec. 2017.
[5] Y. Wei, J.-K. Zhang, and Z. Lu, "A novel successive cancellation method to retrieve sea wave components from spatio-temporal remote sensing image sequences," *Remote Sens.*, vol. 8, no. 7, p. 607, Jul. 2016.
[6] J. Nieto-Borge, P. Jarabo-Amores, D. de la Mata-Moya, and K. Hessner, "Signal-to-noise ratio analysis to estimate ocean wave heights from X-band marine radar image time series," *IET Radar, Sonar Navigat.*, vol. 2, no. 1, pp. 35–41, Feb. 2008.
[7] F. Xu, X. Li, P. Wang, J. Yang, W. G. Pichel, and Y.-Q. Jin, "A backscattering model of rainfall over rough sea surface for synthetic aperture radar," *IEEE Trans. Geosci. Remote Sens.*, vol. 53, no. 6, pp. 3042–3054, Jun. 2015.
[8] N. Braun, M. Gade, and P. A. Lange, "The effect of artificial rain on wave spectra and multi-polarisation X band radar backscatter," *Int. J. Remote Sens.*, vol. 23, no. 20, pp. 4305–4323, Jan. 2002.
[9] J.-S. Lee, "Refined filtering of image noise using local statistic," *Comput. Graph. Image Process.*, vol. 15, no. 4, pp. 380–389, Apr. 1981.
[10] J. Shen, Y. Li, Y. Dai, and S. Wang, "Identification and suppression of rain interference on X-band radar images," *Opt. Precis. Eng.*, vol. 20, no. 8, pp. 1846–1853, Aug. 2012.
[11] B. Lund, H. C. Graber, and R. Romeiser, "Wind retrieval from shipborne nautical X-band radar data," *IEEE Trans. Geosci. Remote Sens.*, vol. 50, no. 10, pp. 3800–3811, Oct. 2012.
[12] Z. Chen, Y. He, B. Zhang, and Y. Ma, "A method to correct the influence of rain on X-band marine radar image," *IEEE Access*, vol. 5, pp. 25576–25583, 2017.

[13] W. Huang, Y. Liu, and E. Gill, "Texture-analysis-incorporated wind parameters extraction from rain-contaminated X-band nautical radar images," *Remote Sens.*, vol. 9, no. 2, p. 166, Feb. 2017.
[14] X. Chen, W. Huang, C. Zhao, and Y. Tian, "Rain detection from X-band marine radar images: A support vector machine-based approach," *IEEE Trans. Geosci. Remote Sens.*, early access, 2019, doi: 10.1109/TGRS.2019.2953143.
[15] H. Zhao, R. Zhang, N. Wu, and X. Hu, "Analysis of sea clutter characteristics based on measured data," *Radar Sci. Technol.*, vol. 7, no. 3, pp. 214–218, Jun. 2009.
[16] J. Zhao, Y. Fu, and W. Geng, "Analysis of sea clutter statistical characteristics," *Mod. Radar*, vol. 27, no. 11, pp. 4–6, Nov. 2005.
[17] Y. Yuan, H. Zhu, Q. Wang, W. Yuan, and N. Yuan, "Correlation feature-based detector for range distributed target in sea clutter," *EURASIP J. Adv. Signal Process.*, vol. 2018, p. 25, Dec. 2018.
[18] Y. Zhang, Z. Deng, J. Shi, Y. Zhang, and H. Liu, "Sea clutter modeling using an autoregressive generalized nonlinear-asymmetric GARCH model," *Digit. Signal Process.*, vol. 62, pp. 52–64, Mar. 2017.
[19] H. Ding, J. Guan, N. Liu, and G. Wang, "New spatial correlation models for sea clutter," *IEEE Geosci. Remote Sens. Lett.*, vol. 12, no. 9, pp. 1833–1837, Sep. 2015.
[20] S. Kemkemian, J.-F. Degurse, V. Corretja, and R. Cottron, "Sea clutter modelling for space-time processing," in *Proc. 17th Int. Radar Symp.*, Krakow, Poland, May 2016, pp. 10–12.
[21] X. Liu, W. Huang, and W. Eric Gill, "Wave height estimation from shipborne X-band nautical radar images," *J. Sensors*, vol. 2016, Jun. 2016, Art. no. 1078053.
[22] Y. Dong and D. Merrett, "Analysis of L-band multi-channel sea clutter," *IET Radar Sonar Navig.*, vol. 4, no. 2, p. 223, 2010.

YAN ZHENG received B.Eng. degree in electronic engineering from the Changchun University of Science and Technology of China, in 2010, and the M.Sc. degree from Harbin Engineering University, in 2014, where he is currently pursuing the Ph.D. degree.

His research areas cover marine radar image processing and analysis, and computer software engineering.

ZHEN SHI received the B.Sc. degree from the Harbin Shipbuilding Engineering Institute, in 1982, and the M.Sc. and Ph.D. degrees from Harbin Engineering University, in 1986 and 2001, respectively.

From 2002 to 2004, he worked at the Mechanical Engineering Postdoctoral Station, Harbin Institute of Technology. He has been engaged in teaching and scientific research at the Department of Aerospace Engineering, College of Mechanical and Electrical Engineering, and College of Automation. He is currently a Professor with the College of Automation, Harbin Engineering University. His main research interests include marine radar image processing, control theory, and control engineering.

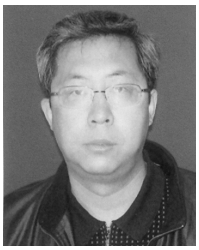

ZHIZHONG LU received the B.Sc. degree from Fudan University, in 1989, the M.Sc. degree from Harbin Engineering University, in 2001, and the Ph.D. degree from Harbin Engineering University, in 2008. He is currently a Professor with the College of Automation, Harbin Engineering University. His main research interests are in marine integrated hydrological remote sensing and information forecasting technology.

WENFENG MA received the B.Sc. degree from the College of Electrical Technology, Harbin University of Science and Technology of China, in 2001.

He is currently with FAWCar Company, Ltd., China. His research areas cover speech recognition, pattern recognition infotainment, and telematics.